Protein Science (1999), *8*:291–297. Cambridge University Press. Printed in the USA.

Crystal structure of human muscle aldolase complexed with fructose 1,6-bisphosphate: Mechanistic implications

ANDREW DALBY,[1] ZBIGNIEV DAUTER,[2,3] AND JENNIFER A. LITTLECHILD[1]

[1]Departments of Chemistry and Biological Sciences, Exeter University, Stocker Road, Exeter EX4 4QD, United Kingdom
[2]EMBL, DESY, D-22603, Hamburg, Germany

(RECEIVED August 12, 1998; ACCEPTED October 28, 1998)

Abstract

Fructose 1,6-bisphosphate aldolase catalyzes the reversible cleavage of fructose 1,6-bisphosphate and fructose 1-phosphate to dihydroxyacetone phosphate and either glyceraldehyde 3-phosphate or glyceraldehyde, respectively. Catalysis involves the formation of a Schiff's base intermediate formed at the ϵ-amino group of Lys229. The existing apo-enzyme structure was refined using the crystallographic free-*R*-factor and maximum likelihood methods that have been shown to give improved structural results that are less subject to model bias. Crystals were also soaked with the natural substrate (fructose 1,6-bisphosphate), and the crystal structure of this complex has been determined to 2.8 Å. The apo structure differs from the previous Brookhaven-deposited structure (1ald) in the flexible C-terminal region. This is also the region where the native and complex structures exhibit differences. The conformational changes between native and complex structure are not large, but the observed complex does not involve the full formation of the Schiff's base intermediate, and suggests a preliminary hydrogen-bonded Michaelis complex before the formation of the covalent complex.

Keywords: fructose 1,6-bisphosphate aldolase; mechanism; Schiff's base

Fructose 1,6-bisphosphate aldolase (FBP aldolase) is an enzyme of the glycolytic pathway that catalyzes the reversible cleavage of fructose 1,6-bisphosphate and fructose 1-phosphate to dihydroxyacetone phosphate and either glyceraldehyde 3-phosphate or glyceraldehyde, respectively (Rutter, 1964).

The FBP aldolases form a subgroup of the larger lyase group of enzymes—the aldolases. The aldolases can be divided into two classes of enzyme, depending on the method of enzyme catalysis. The type I enzymes have a mechanism that involves the formation of a covalent Schiff's base intermediate between the sugar and the enzyme. The type II enzymes are metal-containing enzymes where the substrate is coordinated to a divalent metal cation such as magnesium or ferric iron (Morse & Horecker, 1968).

Reprint requests to: Jennifer A. Littlechild, Departments of Chemistry and Biological Sciences, Exeter University, Stocker Road, Exeter EX4 4QD, United Kingdom; e-mail: JALittlechild@exeter.ac.uk.

[3]Current address: Brookhaven National Laboratory, Upton, New York 11973-5000.

Abbreviations: Asp, aspartic acid; DHAP, dihydroxyacetone phosphate; FBP, fructose 1,6-bisphosphate; FBP aldolase, fructose 1,6-bisphosphate aldolase; F1P, fructose 1-phosphate; Glu, glutamic acid; G3P, glyceraldehyde 3-phosphate; Lys, lysine; PDB, Brookhaven Protein Data Bank; RMSD, root-mean-square deviation.

Type I FBP aldolase is principally found in eukaryotes, with the type II form being the predominant form in bacteria and archaea, but both forms have been found in all three kingdoms, and some organisms possess enzymes of both types (Marsh & Lebherz, 1992).

Mammalian FBP aldolases can further be subdivided into tissue-specific isozymes, which have different substrate specificity. The A isozyme is present in muscle tissue and erythrocytes, and has a higher substrate specificity for fructose 1,6-bisphosphate over fructose 1-phosphate. The B isozyme is found in the liver and reacts with both substrates without preference. This is possibly an indication of the enzymes role in the liver being gluconeogenesis rather than glycolysis. The third (C) isozyme is found in the brain, and is similar to the A isozyme (Penhoet et al., 1966, 1969).

The structures of the type I FBP aldolases from human muscle, rabbit muscle, and *Drosophila melanogaster* have all been determined (Sygusch et al., 1987; Gamblin et al., 1991; Hester et al., 1991). The first type II aldolase structure to be determined was not an FBP aldolase but of L-fuculose-1,5-bisphosphate aldolase. This did not have the same topology as the type I FBP aldolase structures, and so it was believed that the type I and type II aldolase enzymes might be distinguished by the fold that they adopt (Dreyer & Schultz, 1996). The subsequent determination of the structure of the type II FBP aldolase from *Escherichia coli* has shown that this enzyme has the same eight-stranded alpha/beta barrel topology as

the type I FBP aldolases (Blom et al., 1996; Cooper et al., 1996). This is also the topology of the type I aldolase, transaldolase (Jia et al., 1996). A sequence alignment of the L-fuculose-1,5-bisphosphate aldolase with L-ribulose-5-phosphate 4-epimerase has shown a high degree of identity within the N-terminal region of the enzymes (Dreyer & Schultz, 1996). This would suggest that these enzymes are related and that the L-fuculose enzyme is distinct from the other aldolase enzymes that may have evolved from a common ancestor.

A better method of establishing the relationships between these enzymes is an analysis of the active site configuration between the enzymes. It is, therefore, necessary to determine the crystal structure of enzyme–substrate complexes. The structure of a reduced complex of transaldolase with its substrate has already been reported, as well as the binding of dihydroxyacetone phosphate to rabbit muscle aldolase (Blom & Sygusch, 1997; Jia et al., 1997).

Gamblin et al. proposed in modeling studies of the substrate into the crystallographic structure that the phosphates were bound to basic side chains within the barrel (Gamblin et al., 1991). The 1-phosphate site was composed of Arg148 and Lys146, while the 6-phosphate site was composed of Lys41, Arg42, and Arg303. These residues were chosen because of their positions relative to the Schiff's base forming lysine (229), evidence from affinity labeling studies and suggestions from studies of the isozyme specific regions in the sequence (Hartman & Brown, 1978; Takahashi & Hori, 1992). The isozyme studies had suggested that the 6-phosphate region would be different for the A and B isozymes. The 6-phosphate site was, therefore, believed to involve Lys41, in the muscle aldolase that is changed to an asparagine in the liver isozyme.

Other studies have suggested that Lys107 was involved in phosphate binding, and this was supported by site-directed mutagenesis studies that implicated Lys146 in formation/cleavage of the carbon–carbon bond, indicating that it could not be in close proximity to a phosphate group. The alternative phosphate binding sites are summarized by Gefflaut et al. (1995).

The flexible C-terminal region has been implicated in the catalytic mechanism of the enzyme by site-directed mutagenesis, affinity labeling, and chimerical isozyme studies (Kochman & Dobryszycki, 1991; Takahashi & Hori, 1992). This region was not identified in the electron density for the first X-ray crystallographic structure, from rabbit muscle. The structure of human muscle FBP aldolase and that from *D. melanogaster* both have coordinates for this region (Gamblin et al., 1991; Hester et al., 1991). There is a considerable difference between the two structures in this region. This may result from crystal packing, as this is a surface loop of the protein. The rabbit muscle enzyme crystals were shown to be catalytically active, but underwent a change in crystal arrangement during catalysis (Sygusch & Beaudry, 1984). This was detected by a change in the space group of the crystal. It is possible that this results from the motion of this large flexible region during catalysis.

The X-ray crystallographic structure of human muscle aldolase has been re-examined using improved methods of refinement and map generation; in particular, refinement now uses the crystallographic free-*R*-factor. These methods reduce model bias and improve positioning of regions of the protein where there is a large degree of motion. This improved *apo* structure was then used to solve the structure of the enzyme complexed with fructose 1,6-bisphosphate to 2.8 Å resolution. These structures define unequivocally the substrate-binding site for FBP aldolase. This can then be used to investigate the relationship between the aldolase enzymes.

Results and discussion

Refinement of the apo-enzyme model

The high-resolution model was refined from an initial molecular replacement solution using the rabbit muscle aldolase coordinates as the search model. The residues beyond proline 344 were omitted in the rabbit muscle aldolase model, as this residue marks the lower boundary of the flexible C-terminal region. The later stages of refinement used maximum likelihood methods within the REFMAC program and so the calculated maps are of the form 2mfo-fc. It is, therefore, possible to contour these maps at lower sigma than usual. The maps for the C-terminal region generally show continuous density at 1σ, but some side chains and regions near the break in the density could only be contoured at 0.5σ. Even when the density was contoured at 0.5σ, there was no connectivity in the density between residues 345 and 351, and so this region was omitted from the final model.

After manual rebuilding of the protein and associated waters, there were some regions where close contacts remained but where the density made it clear that there was either a water molecule or a strong side-chain–side-chain interaction. Some of the closely associated water molecules could be ammonium ions, as the crystals were grown in ammonium sulfate, but such a complete determination is not possible at this resolution.

The final structure contained 119 water molecules and had an *R*-factor of 17.2% with a free-*R*-factor of 25.8% for the data between 40 and 2.1 Å. There are no residues in either the disallowed regions of the Ramachandran plot or the generously allowed regions. A plot of *B*-factor against residue number is shown in Figure 1. The C-terminal region has particularly high *B*-factors, indicating that it is flexible and may undergo a conformational change on substrate binding.

The flexible C-terminal region

Changes from the previous model of the human muscle aldolase in the core region were minor, and mainly reflected a difference in the side-chain conformations. Differences were much larger for the C-terminal region, and the RMSD in the coordinates for these residues is given in Table 1 as well as the overall, overall side-chain, and overall main-chain deviations. The flexible C-terminal region from Pro344 to Tyr363 has not been found to be in such close proximity to the active site as had been previously proposed. The center of this region does have lower *B*-factors, indicating that Leu356 is involved in an interaction with the core of the protein, which defines the position of the flexible region. This residue is also highly conserved among the aldolase sequences, which suggests this hydrophobic interaction may be particularly important for enzyme activity, and that it is specific in nature.

The enzyme/substrate complex

Crystals of rabbit muscle aldolase remain catalytically active, and this fact has been used to produce a catalytic media by crosslinking micro-crystals with glutaraldehyde (Sobolev et al., 1994). When the rabbit muscle crystals had been soaked with substrate, there was a change in space group, which, along with spectroscopic evidence, suggest that there are motions during catalysis (Sygusch & Beaudry, 1984; Kochman & Dobryszycki, 1991). It was, therefore, expected that in the human muscle aldolase crystals soaked

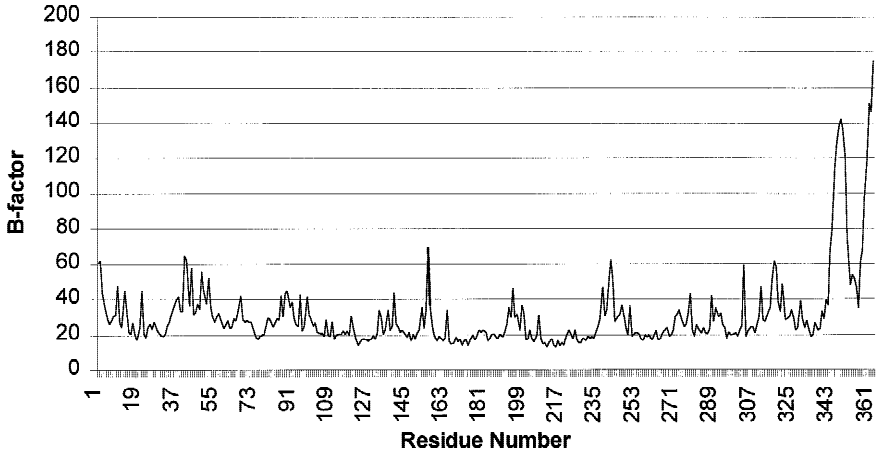

Fig. 1. Plot of *B*-factor against residue number for the native enzyme structure.

with FBP there would be an equilibrium between the substrate and products. The human muscle aldolase crystals grow in a different crystal form to the rabbit muscle enzyme. Density was clearly seen for the substrate from the initial difference map, indicating a high proportion of substrate bound to the enzyme in this crystal form.

The enzyme/substrate complex found in the crystal structure is shown in Figure 2 (PDB accession code 4ald). Due to the limits in the resolution and the almost symmetrical nature of the substrate, FBP was built into to the density in both potential orientations. The best fit of the planar carbonyl to the density during refinement determined the final orientation of the substrate in the model. The complex involves the hydrogen bonding of the phosphate groups to the enzyme and also the close proximity of Lys146 to the C2 carbonyl group. Glu187 is also hydrogen bonded to the C2-carbonyl group of the substrate. The orientation of the substrate within the complex is significantly different from that originally proposed in modeling studies by Gamblin et al., but is in good agreement with the binding of DHAP to rabbit muscle aldolase (Gamblin et al., 1991; Blom & Sygusch, 1997). This Michaelis complex shows the orientation of the phosphate groups and allows unambiguous determination of both phosphate binding sites. The 1-phosphate is associated with the main-chain nitrogens of Ser271 and Gly272. The interaction between two adjacent main-chain nitrogens indicates a strained conformation of the protein backbone at this position. Both of these amino acids are conserved throughout the type I aldolase sequences. A comparison of the phosphate binding sites of other α/β barrels has also shown these enzymes to contain a glycine–glycine or serine–glycine pairing of adjacent amino acids (Bork et al., 1995). This analysis was for enzymes that bound heterocyclic phosphates such as FMN. In all of these enzymes, the phosphate-binding site is close to the C-terminal region of the protein between strand seven and helix eight. A serine–glycine motif is present in the metal containing type II aldolases between strand seven and helix eight, suggesting that this is may be the phosphate-binding site (Cooper et al., 1996).

The flexible C-terminal tail of the molecule is also defined in the complex structure, although it is at lower resolution, but its exact role in catalysis cannot be determined unequivocally from this complex structure, as it is not in close proximity to the substrate. The improved electron density and lower *B*-factors in the complex structure show that this region becomes less flexible on binding of the substrate. There is also some indication that the motion of this C-terminal region covers over the entrance to the active site. This could be to exclude solvent, or with a tighter association residues could be involved in catalysis itself, as suggested by site-directed mutagenesis and phosphorylation studies (Takahashi et al., 1989; Sygusch et al., 1990).

Table 1A. *RMSD in Å for the flexible C-terminal region*

Residue	Main-chain RMSD (Å)	Side-chain RMSD (Å)
Pro344	2.81	3.22
Ala351	15.14	18.29
Ala352	11.23	13.08
Ser353	5.93	6.69
Glu354	4.91	11.21
Ser355	4.04	7.13
Leu356	4.22	7.16
Phe357	3.39	9.77
Val358	2.96	6.11
Ser359	2.23	4.78
Asp360	2.99	7.03
His361	6.57	9.79
Ala362	10.84	13.17
Tyr363	11.71	13.93

Table 1B. *Overall RMS displacements between the original apo-enzyme model and the new structure*

	RMSD (Å)	1.527
Main chain	Average displacement (Å)	0.531
	Maximum displacement (Å)	16.37
	RMS displacement (Å)	2.337
Side chain	Average displacement (Å)	1.049
	Maximum displacement (Å)	18.292

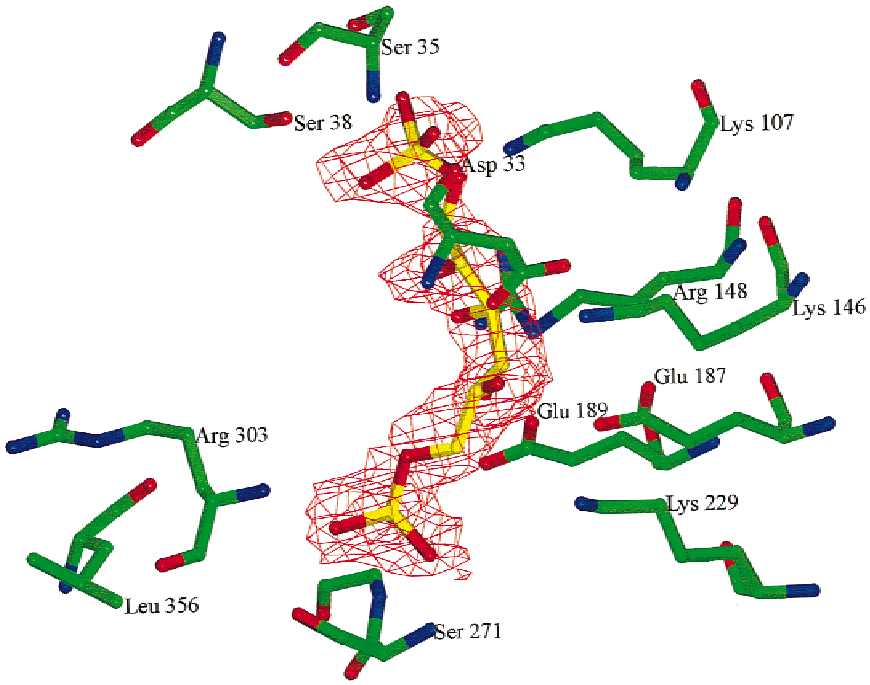

Fig. 2. The active site of human muscle aldolase depicting amino acids involved in the catalytic mechanism. The electron density is a $2f_o - f_c$ map for fructose 1,6-bisphosphate in the enzyme complex structure, contoured at σ.

Comparison with mutagenesis studies

Site-directed mutagenesis, borohydride reduction, and affinity studies have been carried out on a number of residues about the active site. The results from these studies are summarized in Table 2. The determination of the structure of the enzyme–substrate complex has suggested some different interpretations as to the function of the catalytic residues, not possible from the biochemical studies.

The function of the two lysines, Lys229 and Lys107, had been unambiguously determined by the previous mechanistic studies. Lys229 has been determined to be the Schiff's base forming lysine, although the structure does not contain a Schiff's base. This ϵ-nitrogen of the lysine is also in the proximity of Glu187. The glutamic acid may be involved in the deprotonation of the Schiff's base forming lysine, this residue is also in close proximity to the hydroxyl group on C3 of the sugar, and this would suggest that it is both important for orientating the lysine and stabilizing the charges during Schiff's base formation. Lys107 was correctly determined to form part of the 6-phosphate binding site.

Glu189, Lys146, and Arg148 all lie close to the cleavage point in the substrate. Lys146 has interactions with both the C3 and C4 carbons, as does Arg148. The lysine and the arginine had previously been incorrectly associated with the 1-phosphate binding site, providing a positively charged patch in the cleft to bind the negatively charged phosphate. Lys146 also has a close association with Asp33; this acidic residue is also aligned with the C5 hydroxyl group of the substrate. This would suggest that the interaction of the lysine with the substrate involves the deprotonated form. Glu189 has a similar role to that of Glu187 in an electrostatic association with the hydroxyl group on C3 of the sugar.

Arg303 is associated with the 1-phosphate binding site and also with Leu356. These interactions are hydrophobic in nature and not dependent on the terminal nitrogen groups. The interaction with Leu356 seems to play an important role in positioning the flexible C-terminal loop during catalysis. Finally, Tyr363 and His361 seem to have no clear interaction with the substrate. It is possible that this tail region is involved in burying the substrate in a more hydrophobic environment as the tyrosine is directed toward the 6-phosphate group. It is also possible that this region may be involved in some other part of the catalytic mechanism; the cleavage of the furanose ring is a possibility, as this has already occurred before formation of this particular complex (Rose & O'Connell, 1977).

Table 2. *Mutagenesis and chemical modification studies on the type I FBP aldolase mechanism*

Residue	Function	Reference
Asp33	Proton abstraction from C4	Morris and Tolan (1993)
Lys107	6-Phosphate binding	Anai et al. (1973)
Lys146	1-Phosphate binding	Hartman and Brown (1978)
	Stabilizing intermediates	Gupta et al. (1993)
		Morris and Tolan (1994)
Arg148	1-Phosphate binding	Lobb et al. (1976)
Lys229	Schiff's base formation	Lai et al. (1974)

Comparison of the FBP aldolase and transaldolase mechanisms

Jia et al. have shown that FBP aldolase and transaldolase can be structurally aligned (Jia et al., 1996). Both enzymes are Schiff's

Table 3. *Comparison of important residues in the different mechanistic models*

	Original mechanism (Gamblin et al., 1991)	Transaldolase	FBP aldolase residues suggested by enzyme alignment with transaldolase
Schiff's base	Lys229	Lys132	Lys229
Catalytic acid	Asp33	Glu96	Glu187
Catalytic base C3–C4 cleavage	Tyr363	Asp17	Asp33
Deprotonation of Schiff's base	Lys146	—	—

base-forming enzymes, and so an alignment can be made by superimposing the Schiff's base forming lysines. The resulting alignment gives different relative positions of the catalytic amino acids within the fold of the enzyme. It was proposed that this was a result of a cyclic permutation of the gene. An alignment of the two alpha/beta barrels was also possible based on a sequential alignment of the fold. In this case there was less sequence identity in the resulting alignment the Schiff's base-forming lysine was aligned to another lysine, Lys146 in FBP aldolase. Comparison of the enzyme–substrate complexes for both enzymes can now be made and the proposed mechanisms compared.

An alignment of the principal amino acids involved in catalysis from FBP aldolase and transaldolase based on alignments of the Schiff's base-forming lysines, compared with the amino acids assigned catalytic function in the initial FBP aldolase mechanism is given in Table 3.

From the structure of the FBP aldolase complex, Glu187 is also involved in interactions with the substrate and is clearly involved in catalysis. The function of Asp33 is less clear. It is not within hydrogen bonding distance of FBP, but does make contacts with Lys107 and Lys146. Lys107 is also involved with binding the 6-phosphate group, and so these interactions may delocalize the charges from the phosphate group.

Lys146 has been shown to form a Schiff's base with sterically hindered substrates (Blonski et al., 1997), and also in the case of paracatalytic inactivation using borohydride reduction (Gupta et al., 1993). This increases the ambiguity of the structural alignment of the two enzymes as there are now two potential Schiff's base lysines in FBP aldolase that could be aligned. Lys146 has been associated with the deprotonation the Schiff's base forming lysine (Lys229) under normal reaction conditions. The alignment with transaldolase suggests this need not be the case.

The evolutionary relationships between the alpha/beta barrel aldolase enzymes are complex and subtle, and require a more detailed elucidation of the catalytic mechanism than is currently possible.

Materials and methods

Crystallization

Crystals of human muscle aldolase were grown by "hanging" droplet vapor diffusion method using conditions described previously by Millar et al. (1981). Crystals were harvested in mother liquor containing 70% ammonium sulfate in imidazole buffer pH 6.0. Substrate soaks were carried out by the addition of fructose 1,6-bisphosphate to a final concentration of 100 mM and left for several days. These crystals were isomorphous to those of the native enzyme.

Data collection

Both native and substrate soak datasets were collected at the Hamburg Synchrotron on beamline X31 at room temperature. The data were processed using MOSFLM for the high-resolution data set and DENZO for the substrate complex dataset (Leslie, 1992; Otwinowski & Minor, 1997). The statistics for the datasets and their refinement are given in Table 4.

Refinement of the apo-enzyme model

The model of the apo-enzyme was rebuilt using the free-*R*-factor as an improved criterion for refinement (Brünger, 1993). For this to be valid, and for the free-*R* value not to be affected by previous refinement cycles, it was necessary to begin the refinement from the original molecular replacement solution using the rabbit muscle enzyme as the search model. In this case the solution of the molecular replacement problem is trivial, because of the very high

Table 4. *Statistics for data collection and refinement of the native and complex structures*

	Native dataset	Complex dataset
Space group	$P6_422$	$P6_422$
Unit cell parameters	$a = b = 96.50$	$a = b = 96.50$
	$c = 166.90$	$c = 166.90$
	$\alpha = \beta = 90°$	$\alpha = \beta = 90°$
	$\gamma = 120°$	$\gamma = 120°$
Resolution range	19.68–2.10 Å	19.56–2.80 Å
Completeness	78.7%	93.7%
R_{merge}	6%	7%
Redundancy	4.0	4.0
B overall	30.1 Å^2	37.3 Å^2
R-factor for all reflections	0.172	0.226
R-factor $F > 2\sigma$	0.162	0.206
Resolution higher than 5 Å		
Free-*R*-factor	0.258	0.299
No. of atoms in asymmetric unit	2,906	2,783
No. of waters	143	0

identity between the two enzymes (there are only four amino acid differences in the structurally conserved core region).

At this resolution it was also possible to build waters into the density. These were added automatically using ARP (Lamzin & Wilson, 1993). An analysis of the close contacts was used to remove erroneous waters interactively using "O" (Jones et al., 1991). The principal method of refinement was least-squares refinement using the PROLSQ program within the CCP4 suite of programs (CCP4, 1994). As an attempt to improve the poor region of density between residues 345 and 351 an XPLOR simulated annealing simulation was performed with a 15 Å sphere about this region being omitted (Brünger, 1992). There was, however, no improvement in the density for this disordered region, and the atoms for this region were given zero occupancy in the final model (they were retained for modeling purposes). Maximum likelihood methods were used for the final stages of refinement within the REFMAC program (Murshudov et al., 1997). Free-*R*-factor was used throughout as a measure of the progress of the refinement. For the free-*R*-factor, 5% of the data had been selected across all resolution ranges. Atomic *B*-factors were refined isotropically as at this resolution anisotropic refinement is not possible.

Refinement of the enzyme–substrate complex

Difference Fourier maps were calculated using REFMAC, with the calculated phases and amplitudes from the refined high-resolution model and the experimental amplitudes from the substrate soaked crystals. In the initial difference map, density was clearly visible for the substrate, and one of the phosphate sites could be clearly identified. Subsequent refinement also used REFMAC, and the model was rebuilt using "O." *B*-factors were refined per residue due to the limited resolution of the data and the free-*R*-factor calculated using 5% of the data.

The REFMAC restraints for the substrate were determined from a modeled set of coordinates for the substrate created using the InsightII molecular modeling package (Insight User Guide, 1992). This was necessary because the existing crystallographic structures all contained fructose 1,6-bisphosphate in a cyclic form, and in this structure the furanose ring has been cleaved. A dictionary for the substrate was created using the MAKEDICT program (P.R. Evans, pers. comm.). At this resolution it is not possible to reliably build waters, and so the waters were omitted from the enzyme–substrate model. Strict stereochemical restraints were used during the refinement, as if these were relaxed the free-*R*-factor rose. The resulting substrate geometry agreed well with the density, such that the planar carbon of the sugar can be clearly identified.

The density for the disordered region of the structure was much clearer than in the apo-enzyme structure, and no atoms were omitted from the final set of coordinates.

Acknowledgments

The authors are grateful to the European Union for support of the work at the EMBL Hamburg through the HCMP Access to Large Installations Project, Contract number CHGE-CT93-0040. J.A.L. acknowledges the support of the Wellcome Trust in this work.

References

Anai M, Lai CY, Horecker BL. 1973. Pyridoxal phosphate binding site of rabbit muscle aldolase. *Arch Biochem Biophys 156*:712–719.

Blom NS, Sygusch J. 1997. Product binding and role of the C-terminal region in class I D-fructose-1,6-bisphosphate aldolase. *Nat Struct Biol 4*:36–39.

Blom NS, Tetreault S, Coulombe R, Sygusch J. 1996. Novel active site in *Escherichia coli* fructose-1,6-bisphosphate aldolase. *Nat Struc Biol 3*:856–862.

Blonski C, De Moissac DD, Périe J, Sygusch J. 1997. Inhibition of rabbit muscle aldolase by phosphorylated aromatic compounds. *Biochem J 323*:71–77.

Bork P, Gellerich J, Groth H, Hooft R, Martin F. 1995. Divergent evolution of a β/α-barrel subclass: Detection of numerous phosphate-binding sites by motif search. *Protein Sci 4*:268–274.

Brünger AT. 1992. *X-PLOR manual*, version 3.1. New Haven, Connecticut: Yale University Press.

Brünger AT. 1993. Assessment of phase accuracy by cross validation: The free *R* value. Methods and applications. *Acta Crystallogr A42*:140–149.

CCP4, The Collaborative Computational Project, No. 4. 1994. The CCP4 suite: Programs for protein crystallography. *Acta Crystallogr D50*:760–763.

Cooper SJ, Leonard GA, McSweeney SM, Thompson AW, Naismith JH, Qamar A, Plater A, Berry A, Hunter WH. 1996. The crystal structure of a class II fructose-1,6-bisphosphate aldolase shows a novel binuclear metal-binding active site embedded in a familiar fold. *Structure 14*:1303–1315.

Dreyer MK, Schultz GE. 1996. The spatial structure of the class II L-fuculose-1-phosphate aldolase from *Escherichia coli*. *Acta Crystallogr D52*:1082–1091.

Gamblin SJ, Davies GJ, Grimes JM, Jackson RM, Littlechild JA, Watson HC. 1991. Activity and specificity of human aldolases. *J Mol Biol 219*:573–576.

Gefflaut T, Blonski C, Perie J, Willson M. 1995. Class I aldolases: Substrate specificity, mechanism, inhibitors and structural aspects. *Prog Biophys Mol Biol 63*:301–340.

Gupta S, Hollenstein R, Kochbar S, Christen P. 1993. Paracatalytic inactivation of fructose 1,6-bisphosphate aldolase. *Eur J Biochem 214*:515–519.

Hartman FC, Brown JP. 1978. Affinity labelling of a previously undetected lysyl residue in class I aldolase. *J Biol Chem 251*:3057–3062.

Hester G, Brenner-Holzach O, Rossi FA, Struck-Donatz M, Winterhalter KH, Smit JG, Piontek K. 1991. The crystal structure of fructose 1,6-bisphosphate aldolase from *Drosophila melanogaster* at 2.5 angstrom resolution. *FEBS Lett 292*:237–242.

Insight user guide, version 2.1.0. 1992. San Diego: Biosym Technologies.

Jia J, Huang W, Schörken U, Sahm H, Sprenger GA, Lindqvist Y, Schneider G. 1996. Crystal structure of transaldolase from *Escherichia coli* suggests a circular permutation of the α/β barrel within the class I aldolase family. *Structure 4*:715–724.

Jia J, Schörken U, Lindqvist Y, Sprenger GA, Schneider G. 1997. Crystal structure of the reduced Schiff-base intermediate complex of transaldolase B from *Escherichia coli:* Mechanistic implications for class I aldolases. *Protein Sci 6*:119–124.

Jones TA, Zou JY, Cowan S, Kjeldgaard M. 1991. Improved methods for building protein models in electron density maps and location of errors in these models. *Acta Crystallogr A47*:110–119.

Kochman M, Dobryszycki P. 1991. Topography and conformational changes of fructose-1,6-bisphosphate aldolase. *Acta Biochim Pol 38*:407–421.

Lai C, Nakai N, Chang D. 1974. Amino acid sequence of rabbit muscle aldolase and the structure of the active site. *Science 183*:1204–1206.

Lamzin VS, Wilson KS. 1993. Automated refinement of protein models. *Acta Crystallogr D49*:129–147.

Leslie AGW. 1992. Recent changes to the MOSFLM package for processing film and image plate data. In: *Joint CCP4 and ESFEACMB newsletter on protein crystallography. No. 24. SERC.* Warrington, UK: Daresbury Laboratory.

Lobb RR, Stokes AM, Hill HAO, Riordan JF. 1976. Arginine as the C-1 phosphate binding site in rabbit muscle aldolase. *FEBS Lett 54*:70–72.

Marsh JJ, Lebherz HG. 1992. Fructose–bisphosphate aldolases: An evolutionary biology. *Trends Biosci 17*:110–113.

Millar JR, Shaw PJ, Stammers DK, Watson HC. 1981. The low resolution structure of human muscle aldolase. *Philos Trans R Soc Lond B 293*:209–214.

Morris AJ, Tolan DR. 1993. Site directed mutagenesis identifies Asp 33 as a previously unidentified critical residue in the catalytic mechanism of rabbit aldolase A. *J Biol Chem 268*:1095–1102.

Morris AJ, Tolan DR. 1994. Lysine 146 of rabbit muscle aldolase is essential for the cleavage and condensation of the C3-C4 bond of fructose 1,6-bisphosphate. *Biochemistry 33*:12291–12297.

Morse DE, Horecker BL. 1968. The mechanism of action of aldolases. *Adv Enzymol 31*:125–181.

Murshudov GN, Vagin AA, Dodson EJ. 1997. Refinement of macromolecular structures by the maximum likelihood method. *Acta Crystallogr D53*:240–255.

Otwinowski Z, Minor W. 1997. Processing of X-ray diffraction data collected in oscillation mode. *Methods Enzymol 276*:307–326.

Penhoet EE, Kochman M, Rutter WJ. 1969. Molecular and catalytic properties of human aldolase C. *Biochemistry 8*:4396–4402.

Penhoet EE, Rajkumar T, Rutter WJ. 1966. Multiple forms of aldolase in mammalian tissues. *Proc Natl Acad Sci USA 56*:1275–1282.

Rose IA, O'Connell EL. 1977. Specificity of fructose-1,6-P_2 aldolase (muscle) and partition of the enzyme among catalytic intermediates in the steady state. *J Biol Chem 253*:479–482.

Rutter WJ. 1964. The evolution of aldolase. *Fed Proc 23*:1248–1257.

Sobolev SB, Bartoszko-Malik A, Oeschger TR, Montelbano MM. 1994. Cross-linked enzyme crystals of fructose diphosphate aldolase: Development as a catalyst for synthesis. *Tetrahedron Lett 35*:7751–7754.

Sygusch J, Beaudry D. 1984. Catalytic activity of rabbit skeletal muscle aldolase in the crystal state. *J Biol Chem 259*:10222–10227.

Sygusch J, Beaudry D, Allaire M. 1987. Molecular architecture of rabbit skeletal muscle aldolase at 2.7 angstrom resolution. *Proc Natl Acad Sci USA 84*:7846–7850.

Sygusch J, Beaudry D, Allaire M. 1990. Inactivation of mammalian fructose diphosphate aldolases by COOH terminus autophosphorylation. *Arch Biochem Biophys 283*:227–233.

Takahashi I, Takasaki Y, Hori K. 1989. Site directed mutagenesis of human aldolase isozymes: The role of cys. 72 and cys. 338 residues of aldolase A and the carboxy-terminal tyr residues of aldolase A and B. *J Biochem 105*:281–286.

Takahashi I, Hori K. 1992. Studies on chimeric fusion proteins of human aldolase isozymes A and B. *Protein Eng 5*:101–104.